Available online at www.sciencedirect.com
ScienceDirect
Lithos 96 (2007) 266–280
LITHOS
www.elsevier.com/locate/lithos

Triassic collision of western Tianshan orogenic belt, China: Evidence from SHRIMP U–Pb dating of zircon from HP/UHP eclogitic rocks

Lifei Zhang [a,b,*], Yongliang Ai [a], Xuping Li [a], Daniela Rubatto [c,d], Biao Song [b], Samantha Williams [c], Shuguang Song [a], David Ellis [c], J.G. Liou [e]

[a] *The Key Laboratory of Orogenic Belt and Crustal Evolution, MOE; School of Ear th and Space Sciences, Peking University, China*
[b] *Beijing SHRIMP Center, CAGS, China*
[c] *Department of Earth and Marine Sciences, Australian National University, Canberra, 0200 Australia*
[d] *Research School of Earth Sciences, Australian National University, Canberra, 0200 Australia*
[e] *Department of Geological and Environmental Sciences, Stanford University, USA*

Received 26 November 2005; received in revised form 11 May 2006; accepted 15 September 2006
Available online 29 December 2006

Abstract

A newly recognized ultrahigh-pressure (UHP) terrane in the Chinese Western Tianshan orogenic belt contains blueschists, eclogites and metapelites. This belt extends westward to the "South Tianshan" in Tajikistan, Kyrgyzstan, Kazakhstan and Uzbekistan for more than 2500 km long in central Asia. New ion microprobe (SHRIMP) U–Pb dating of zircon from HP-UHP eclogites and metapelites indicates Triassic ages for the collision in western Tianshan. Zircon from four eclogites yields magmatic ages of 310–413 Ma in the cores and one metapelite contained detrital zircon cores as old as 1886±20 Ma. Zircon rims reveal the HP-UHP metamorphic ages of 233±4–226±4.6 Ma. The geochronologial data suggest that a South Tianshan paleo-ocean was developed between the Tarim continent and the Yili-central Tianshan Craton before the Carboniferous (>310 Ma). During the Permian–Triassic subduction and continent collision, oceanic basalts underwent HP/UHP metamorphism. A new tectonic model for HP-UHP metamorphic rocks of the Chinese Western Tianshan orogenic belt represented by HP-UHP metamorphic eclogitic rocks is proposed in the light of recent paleomagnetic, paleontologic, sedimentary and stratigraphic studies.

Keywords: Triassic collision; SHRIMP U–Pb zircon geochronology; HP-UHP metamorphic belt; Chinese western Tianshan

1. Introduction

The Chinese Tianshan orogenic belt extends for more than 200 km between the Tarim plate to the south and the Yili-central Tianshan craton to the north (Fig. 1). Recently, this orogenic belt composed of blueschists, eclogites and metapelites have been considered as a new ultrahigh pressure metamorphic terrane (Zhang et al., 2002a,b, 2003a,b, 2005). Westward, the Chinese Western Tianshan belt connects with the so called "South Tianshan" in Tajikistan, Kyrgyzstan, Kazakhstan and Uzbekistan forming a more than 2500 km long Central Asia orogenic belt (Sengör et al., 1993; Volkava and

* Corresponding author. The Key Laboratory of Orogenic Belt and Crustal Evolution, MOE; School of Earth and Space Sciences, Peking University, China.
E-mail address: lfzhang@pku.edu.cn (L. Zhang).

0024-4937/$ - see front matter © 2006 Elsevier B.V. All rights reserved.
doi:10.1016/j.lithos.2006.09.012

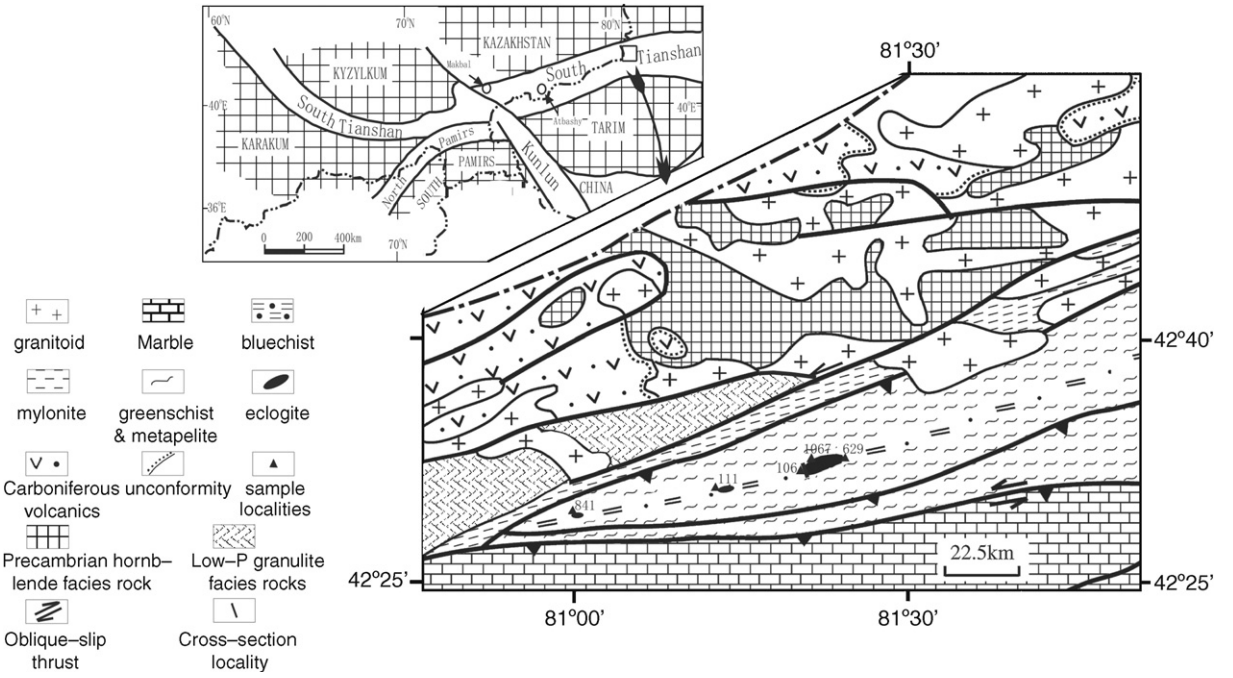

Fig. 1. Geological map of western Tianshan high P/T metamorphic belt, Xinjiang, China (modified after Zhang et al., 2003). (a) shows the distribution of south Tianshan orogenic belt in Eurasian continent (modified after Volkava et al., 1999). Open circle: the localities of coesite pseudomorphs in eclogites from Kazakhstan.

Budanov, 1999). This vast orogenic belt has been extensively investigated as it plays a key role for understanding the geological evolution of the Eurasian continent (Windley et al., 1990; Allen et al., 1992; Sengör et al., 1993). However, the basic problem about the time of collision between the Tarim and Kazakhstan plates, which formed the Tianshan orogenic belt, is poorly constrained. It is usually believed that most of central Asia, including the Tianshan region, was accreted during Paleozoic in central Asia (Windley et al., 1990; Sengör et al., 1993). The present elevation and nearly E–W orientation of the Tianshan belt have been attributed to the collision between the Indian plate and the Eurasian continent during Late Cenozoic (Abdrakhmatov et al., 1996; Allen et al., 1999).

Obtaining precise and accurate ages for orogenic events is an essential for establishing the geological history of a terrane. HP-UHP metamorphic rocks are the most important witnesses of the tectonothermal process that happen during the convergence between different tectonic plates. Therefore, the dating of HP-UHP rocks is a key to understand the formation and evolution of an orogenic belt. It is known that the southwestern Tianshan eclogites associated with blueschist are typical low temperature eclogite (Gao et al., 1999; Zhang et al., 2000), which cannot be easy to get a correct metamorphic age (Thöni, 2002; Jahn et al., 2005). So far, several $^{40}Ar/^{39}Ar$ plateau and Rb/Sr isochron ages and one Sm–Nd isochron age obtained from Chinese Tianshan eclogites and blueschists resulted in Late Paleozoic ages (Gao et al., 2000; Gao and Klemd, 2003; Klemd et al., 2005), but no U–Pb dating geochronology has been carried out. It is known that the development of ion microprobe (e.g., SHRIMP) can give in-situ measurements of U–Pb ages of new growth rims in a single zircon crystal, which may record the exact metamorphic age of the rocks (Rubatto and Gebauer, 2000).

In this paper, we report new ion microprobe (SHRIMP) U–Pb ages of zircon from eclogitic rocks from the Chinese Western Tianshan. This technique allows age measurements on zircon domains that record the magmatic and metamorphic history of the rocks. The data, together with available geological–geophysical evidence, help constraining a new tectonic model for the formation of the Tianshan paleo-ocean, the Late Paleozoic subduction of oceanic and continental materials and the final Triassic collision between the Tarim and Yili-central Tianshan microcontinent.

2. Regional geology and sample description

The Western Tianshan HP-UHP belt is considered to have been formed by the northward subduction of Tarim

plate beneath the Yili-central Tianshan plate (Kazakhstan plate) when the south Tianshan paleo-ocean closed (Windley et al., 1990; Allen et al., 1992; Gao et al., 1999; Zhang et al., 2000). The fault-bounded belt consists mainly of eclogites, blueschists, greenschists and garnet–phengite schists. The northern part consists of low pressure metamorphic rocks and a magmatic arc complex, whereas in the south layers of marbles and chlorite–muscovite-schists occur (Fig. 1). Cordierite–sillimanite biotite gneisses and two-pyroxene granulites of the northern belt yielded SHRIMP U–Pb zircon ages of 290–280 Ma interpreted as dating the low-P metamorphism and the associated arc magmatism (Li and Zhang, 2004).

The eclogites in western Tianshan, China, were first reported by Gao (1997) and Gao et al. (1997). The primary petrography studies were carried out by Gao et al. (1999) and Zhang et al. (2000). Since the inclusions of coesite pseudomophs in garnet, quartz exsolution laminae in omphacite and relict metamorphic magnesite in Tianshan eclogite were reported by Zhang et al. (2002a,b), the UHP metamorphism in western Tianshan was hotly debated (see the comment by Klemd, 2003 and reply by Zhang et al., 2003a). After that, some new UHP minerals such as the coexistence of magnesite and aragonite after dolomite in metapelites (Zhang et al., 2003b), and the relict coesite exsolution laminae in porphyroblastic omphacite in eclogites (Zhang et al., 2005a) were reported subsequently in western Tianshan. So far, three types of HP-UHP eclogites were recognized based on the geological occurrence and petrological feature (Zhang et al., 2000, 2002a). Type I eclogite occurs as blocks, lenses, or layers within pods of mafic blueschists; some of these glaucophane–zoisite eclogites contain inclusions of coesite pseudomorphs in garnet and relict coesite exsolution in omphacite (Zhang et al., 2005). The geochemistry study of trace element shows that their protoliths should be ocean island basalt (OIB) (Ai et al., 2005). Type II eclogite is characterized by preservation of pillow structure, and occurrence of quartz exsolution rods in omphacite (Zhang et al., 2002a). Their characteristics of trace element indicate that their protoliths were probably affinity of enriched mid-ocean ridge basal (E-MORB) (Ai et al., 2005). Type III eclogite is magnesite-bearing banded calcite/dolomite eclogites that occur as lenticular bodies within marbles in which the discovered carbonate reaction of dolomite = magnesite + aragonite indicates the upper limit pressure is lower than 5 GPa (Zhang et al., 2003b). Most rocks have apparently been subjected to ductile deformations; eclogite, blueschist and garnet phengite schist have been intensively compressed. Isoclinal folds, incumbent folds prevail, and the folded rocks are subsequently cut by thrust faults (Fig. 2).

Five eclogite-facies metamorphic rocks in the Western Tianshan HP-UHP belt were selected for SHRIMP U–Pb dating. Three type I eclogite samples (629, 106 and 1067) contain garnet (15–20%), omphacite (30%),

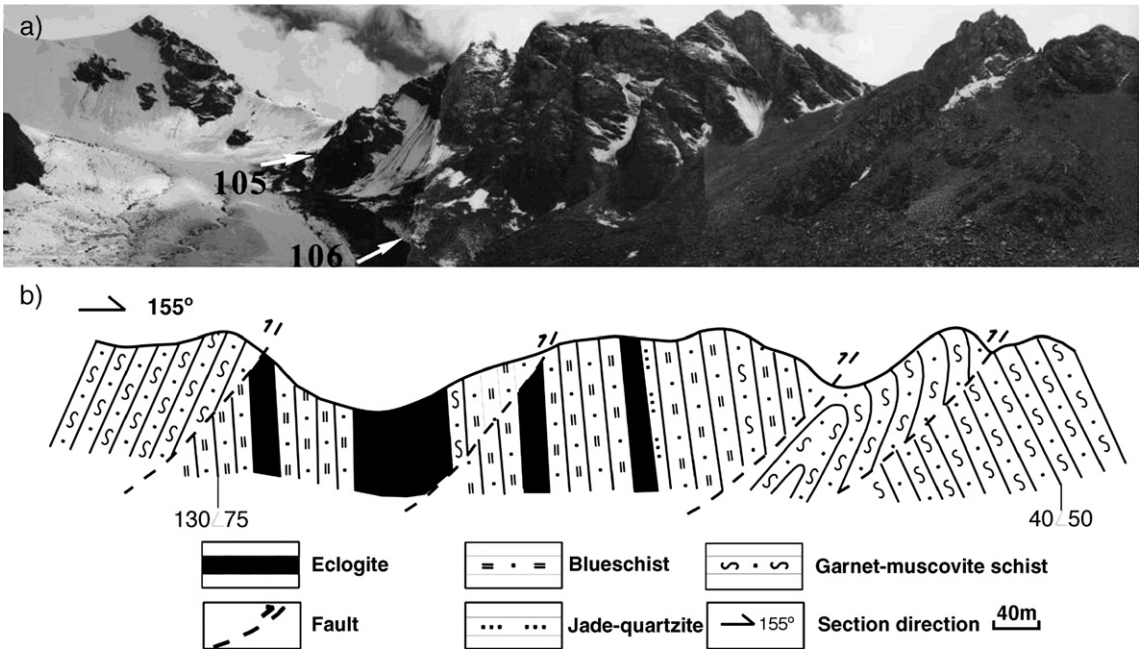

Fig. 2. a. A field view of the cross-section study area. b. A cross-section shows the contact relations of HP-UHP eclogites, blueschists and phengite schists (modified after Zhang et al., 2005b).

glaucophane (10–20%), zoisite (10–15%), carbonate minerals (5–10%), paragonite (5–10%) and minor rutile and titanite with porphyroblastic metamorphic texture. The porphyroblastic garnets with grain size between 0.1 mm and 4 mm have obvious cores crowded with inclusions of omphacite, crossite, zoisite and paragonite. In contrast, the margins contain only inclusions of coesite pseudomophs which is consistent with the prograde compositional zoning of garnet (Zhang et al., 2002a). Some inclusions of mineral association of zoisites and paragonite occurred as box-shaped pseudomophs in porphyroblastic garnet are interpreted to be retrograded from former lawsonite (Zhang et al., 2000). Beside as inclusions in garnet, zoisite also occur as porphyroblastic mineral associated with garnet and omphacite. Carbonate minerals are mainly porphyroblastic dolomite. Paragonite associated with glaucophane occurs as retrograde mineral only in matrix. The relict coesite exsolution rods in porphyroblastic omphacite and coesite pseudomorphs in the margin of garnet proposed that this type eclogites have undergone UHP metamorphic evolution (Zhang et al., 2005a).

One type III eclogite (841) is characterized by more than 30% carbonate mineral, along with garnet (15%), omphacite (20%), glaucophane (20%), zoisite (10%), and paragonite (5%), together with minor rutile and titanite. Porphyroblastic garnet (0.5–1.0 mm) has inclusions of quartz pseudomorphs after coesite (Zhang et al., 2002b). Besides primary glaucophane, garnet rims are replaced by glaucophane and dolomite. Primary omphacite occurs as fine prismatic inclusions within dolomite and as medium grained aggregation of short prismatic crystals associated with garnet replaced by secondary glaucophane. The abundant carbonate minerals are dolomite and magnesite in this kind eclogite. Magnesite occurs only as relic, rounded to subidiomorphic inclusions (0.01 mm–0.1 mm) within dolomite, and as rounded inclusions with thin reaction rims of dolomite within secondary glaucophane (Zhang et al., 2002b). Many carbonate grains have a dark-red oxidized rim due to weathering. These textures indicate clearly two possible mineral generations in this type eclogite, i.e., the peak UHP eclogite facies mineral assemblage of garnet + omphacite + magnesite + coesite, and the retrograde epidote blueschist facies mineral assemblage of dolomite + glaucophane + zoisite. The phase equilibrium calculation on the peak mineral assemblage suggested that the peak metamorphic conditions are 558–597 °C and 3.7–4.0 GPa (Zhang et al., 2002b).

One omphacite–garnet–phengite schist (111) interlayered with type I eclogites and blueschists consists of omphacite (5%), garnet (3%), phengite (45%), quartz (45%) and rutile (2%). In contrast, porphyroblastic garnet in this kind rocks has no any inclusion inside. The matrix minerals are omphacite, phengite and quartz. There are no UHP minerals found in this kind of schist yet. The localities of these samples are shown in Fig. 1.

3. Analytical methods

Zircon separates were prepared using conventional crushing techniques and hand-picked; they were mounted onto epoxy resin discs and polished to expose the grain centers. Crystals of standard zircon AS3 (1099 Ma, Paces and Miller, 1993) and Temora, (417 Ma) were also cast in the mount for analyses at the same conditions in the ANU and Beijing laboratory, respectively. A zircon of known composition (SL13, 238 ppm U) was used as U standard and mounted either with the samples (ANU) or on a separate epoxy (Beijing). The grain mounts were photographed and gold-coated. Assessment of zircon grains and the choice of analytical sites were based on transmitted and reflected light microscopy and cathodoluminescence (CL) imaging. Cathodoluminescence (CL) imaging of sample 841 and 629 was carried out at the Electron Microscopy Unit, Australian National University, on an HITACHI S2250-N scanning electron microscope working at 15 kV, ~60 μA, and ~20 mm working distance. The other samples were analyzed in Beijing with a PHILIPS XL30 SEM in PKU, operating at 15 kV and 120 μA.

Zircon U–Th–Pb analyses were made by SHRIMP II ion-microprobe at the Research School of Earth Sciences (samples 629 and 841), Australian National University and at the Beijing SHRIMP Laboratory, Chinese Academy of Geological Sciences (samples 106, 1067 and 111). Details of the analytical procedure follow Compston et al. (1992), Stern (1998) and Williams (1998). Typically, a 25–30 μm diameter spot was used, with a mass-filtered O_2^+-primary beam of ~5 nA. Data for each spot were collected in sets of 5 (Beijing) or 7 (Canberra) scans through the mass range of Zr_2O^+, $^{204}Pb^+$, Background, $^{206}Pb^+$, $^{207}Pb^+$, $^{208}Pb^+$, $^{238}U^+$, $^{248}ThO^+$, $^{254}UO^+$. The common Pb correction was based on the measured ^{204}Pb (Beijing) or the $^{208}Pb/^{206}Pb$ ratio according to (ANU) (Compston et al., 1984). The Temora and AS3 standard zircon was used for U–Pb calibration, and analyzed after each 3–4 analyses of the unknown samples. The program SQUID developed by Dr. K. Ludwig (2002) was used for data processing, in which the correction formula of Pb/U fractionation is $(^{206}Pb^+/^{238}U^+)/(^{238}U^{16}O^+/^{238}U^+)^b$ (Black et al., 2003). This formula follows the relationship $Pb^+/U^+ = a(UO^+/U^+)^b$ described by Claoué-Long et al. (1995). Results are shown in Table 1 with 2σ errors.

Table 1
U, Th and Pb SHRIMP zircon data of eclogitic rocks from western Tianshan, China

Sample	Domain	U/ppm	Th/ppm	Th/U	% com Pb	$^{206}Pb/^{238}U$	±	$^{207}Pb/^{235}U$	±	Age 206/238	±
1067-1.1	Rim	438	18	0.04	1.22	0.03487	0.0019	0.234	0.094	221.0	4.2
1067-3.1	Core	398	93	0.24	2.60	0.04658	0.0011	0.342	0.091	293.5	3.1
1067-4.1	Core	862	181	0.22	0.50	0.04591	0.0072	0.333	0.040	289.4	2.0
1067-5.1	Rim	379	30	0.08	2.34	0.03709	0.0012	0.218	0.120	234.8	2.7
1067-7.1	Rim	275	12	0.05	2.88	0.03528	0.0014	0.207	0.150	223.5	3.1
1067-9.1	Rim	631	44	0.07	1.33	0.03611	0.0011	0.238	0.110	228.7	2.4
1067-10.1	Rim	591	217	0.38	0.87	0.03664	0.0086	0.266	0.065	232.0	2.0
1067-11.1	Rim	335	3	0.01	1.27	0.03460	0.0012	0.201	0.068	219.3	2.6
1067-12.1	Rim	291	17	0.06	1.10	0.03525	0.0014	0.250	0.110	223.3	3.1
1067-14.1	Rim	350	8	0.02	2.28	0.03353	0.0026	0.216	0.130	212.6	5.4
1067-16.1	Rim	355	12	0.03	0.92	0.03511	0.0011	0.305	0.051	222.5	2.3
106-1.1	Rim	6275	4713	0.78	0.33	0.04146	0.0012	0.295	0.015	261.9	3.0
106-2.1	Rim	6900	5604	0.84	0.26	0.04002	0.0012	0.279	0.015	253.0	2.9
106-2.2	Rim	6024	6510	1.12	0.55	0.04376	0.0011	0.307	0.016	276.1	3.1
106-3.1	Rim	4985	4345	0.90	0.90	0.04204	0.0012	0.299	0.023	265.5	3.0
106-6.1	Rim	3359	2448	0.75	6.05	0.04043	0.0012	0.253	0.079	255.5	3.1
106-9.2	Rim	4787	3332	0.72	0.33	0.04030	0.0012	0.281	0.017	254.7	2.9
106-7.1	Rim	882	505	0.59	0.63	0.03615	0.0016	0.254	0.033	228.9	3.5
106-7.2	Core	161	84	0.54	0.06	0.0662	0.0016	0.540	0.046	413.4	6.3
106-5.1	Rim	505	190	0.39	4.38	0.03608	0.0016	0.261	0.100	228.5	3.7
106-5.2	Rim	1409	544	0.40	1.32	0.04635	0.0012	0.339	0.037	292.1	3.5
106-8.1	Rim	1317	796	0.62	1.09	0.03653	0.0014	0.237	0.038	231.3	3.1
106-9.1	Rim	7208	5553	0.80	0.26	0.03797	0.0012	0.269	0.020	240.2	2.7
106-12.1	Rim	8129	6023	0.77	0.52	0.03744	0.0012	0.262	0.018	237.0	2.7
106-14.1	Rim	1523	666	0.45	1.00	0.03476	0.0013	0.257	0.036	220.3	2.8
629-1.1	Core	122	65	0.53	0.52	0.05059	0.0010	0.347	0.024	318.1	6.2
629-2.1	Core	94	32	0.34	1.93	0.04774	0.0011	0.289	0.029	301.2	7.1
629-3.1	Core	118	56	0.47	1.01	0.04819	0.0011	0.318	0.029	303.2	7.3
629-4.1	Core	51	20	0.39	1.68	0.04963	0.0012	0.354	0.040	312.3	7.4
629-5.1	Core	114	63	0.55	1.36	0.04752	0.0009	0.349	0.026	299.4	5.2
629-6.1	Core	103	50	0.48	0.5	0.04983	0.0010	0.367	0.035	314.2	6.4
629-7.1	Core	145	93	0.64	0.51	0.05026	0.0011	0.367	0.030	316.3	7.3
629-8.1	Core	86	40	0.46	0.62	0.04882	0.0013	0.337	0.031	307.1	8.2
629-9.1	Core	79	42	0.53	0.75	0.05161	0.0013	0.38	0.046	324.4	8.1
629-10.1	Core	98	53	0.54	0.81	0.05014	0.0011	0.365	0.029	315.3	7.2
841-2.1	Core	119	63	0.53	0.33	0.04997	0.0010	0.358	0.041	314.2	6.4
841-3.1	Core	79	37	0.46	1.32	0.04816	0.0011	0.329	0.029	303.1	7.3
841-5.1	Core	84	37	0.43	0.65	0.04819	0.0015	0.347	0.037	303.0	9.1
841-7.1	Core	1136	842	0.74	0.51	0.04976	0.0007	0.359	0.011	313.2	4.0
841-8.1	Core	152	89	0.59	0.63	0.04896	0.0009	0.348	0.027	308.3	5.2
841-1.1	Core	191	244	1.28	1.04	0.0385	0.0007	0.23	0.028	244.4	4.1
111-1.1	Core	2536	168	0.07	0.16	0.3035	0.0029	4.77	0.029	1709.3	44
111-1.2	Rim	1060	34	0.03	0.99	0.0375	0.0030	0.241	0.057	237.0	6.9
111-2.1	Core	2462	188	0.08	0.01	0.2886	0.0029	4.50	0.029	1634	42
111-2.2	Rim	2144	137	0.07	0.19	0.0360	0.0029	0.2610	0.035	228.2	6.6
111-3.1	Core	5303	418	0.08	0.01	0.2755	0.0029	4.31	0.030	1568	41
111-3.2	Rim	1145	25	0.02	0.03	0.0383	0.0030	0.2738	0.034	242.2	7.0
111-4.2	Core	1773	46	0.03	0.66	0.1029	0.0029	1.450	0.031	631	18
111-6.3	Core	959	21	0.02	0.83	0.06940	0.0012	0.787	0.032	432.5	5.1
111-8.1	Core	3825	325	0.09	0.15	0.31310	0.0025	4.893	0.062	1755.9	3.8
111-8.2	Rim	1714	32	0.02	–	0.03665	0.0012	0.2989	0.023	232.0	2.7
111-9.1	Core	4673	208	0.05	0.02	0.24773	0.0029	3.970	0.056	1426.8	3.7
111-7.1	Core	59	68	1.20	0.50	0.0482	0.0027	0.472	0.150	303.6	7.9
111-7.1	Core	2411	141	0.06	0.15	0.27008	0.0029	4.193	0.050	1541.2	3.9
111-9.1	Core	5315	421	0.08	0.04	0.21638	0.0028	3.377	0.040	1262.7	3.2

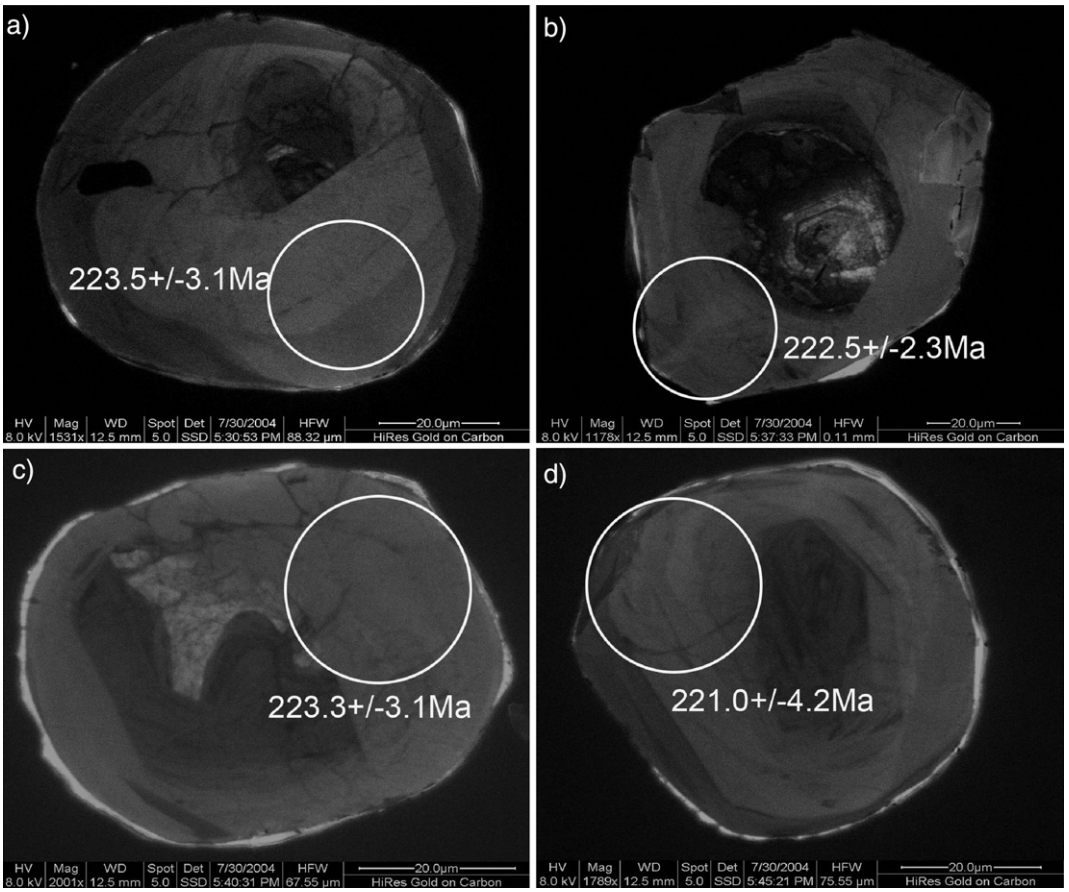

Fig. 3. Representative CL images of rounded zircon crystals for SHRIMP U–Pb analyses from the eclogite 1067 in Western Tianshan, China.

Trace elements in zircons were analyzed in-situ on a Perkin Elmer laser-ablation ICP-MS in the MOE Key Laboratory at the Northwest University, Xi'an (Liu et al., 2002). Laser sampling was done with a pulsed 193 nm ArF Excimer laser with 170 mJ energy at a repetition rate of 10 Hz and pit size of 40 μm. A helium stream was used to transport the sample effectively and reduce deposition at the ablation site. The helium carrier gas inside the ablation cell is mixed with argon as a makeup gas before entering the ICP to maintain stable and optimum excitation conditions (Liu et al., 2002). SiO_2 content of zircon by electron micro-probe analysis was applied as an internal calibration standard, and NIST612 was analyzed twice every 5 analyses as the external standard. Detection limits for most REEs were <0.05 ppm. Repeated analysis of standards yielded precisions better than 10% for most elements.

4. The analyses and U–Pb SHRIMP dating of zircon

The zircons from eclogite sample 1067 are rounded and colorless with 80–100 μm in major dimension. Among the 25 grains selected for analysis, there are 22 grains have core-rim structure on the CL images, i. e., the dark-luminescent core surrounded by a narrow bright-luminescent rim (Fig. 3). Some of the cores have oscillatory-zoning, but no zoning was observed in the rims. A few inclusions of rutile have been found in the rims of zircon associated with garnet and omphacite (Ai, 2005). Nine analyses of zircon rims with Th/U values from 0.01 to 0.08 (except spot 6.1 with 0.22) (Table 1) yield weight mean $^{206}Pb/^{238}U$ ages of 226.3±4.6 Ma. (Fig. 4a). Two analyses of zircon cores gave 289.4± 2.0 Ma and 293.5±3.1 Ma with Th/U values of 0.22 and 0.24 respectively (Fig. 4a). The trace element analyses of zircon crystals show that the content of HREE and Y are higher in the cores (∑HREE: 693–2232 ppm and Y: 990–3129 ppm) than in the rims (∑HREE: 37–122 ppm and Y: 67–145 ppm), and the Eu/Eu* values are smaller in the cores (0.19–0.42) than in the rims (0.42–0.74) (Table 2; Fig. 5a). The low HREE content and the absence of a negative Eu anomaly imply that the zircon rims might have grown concurrently with garnet and

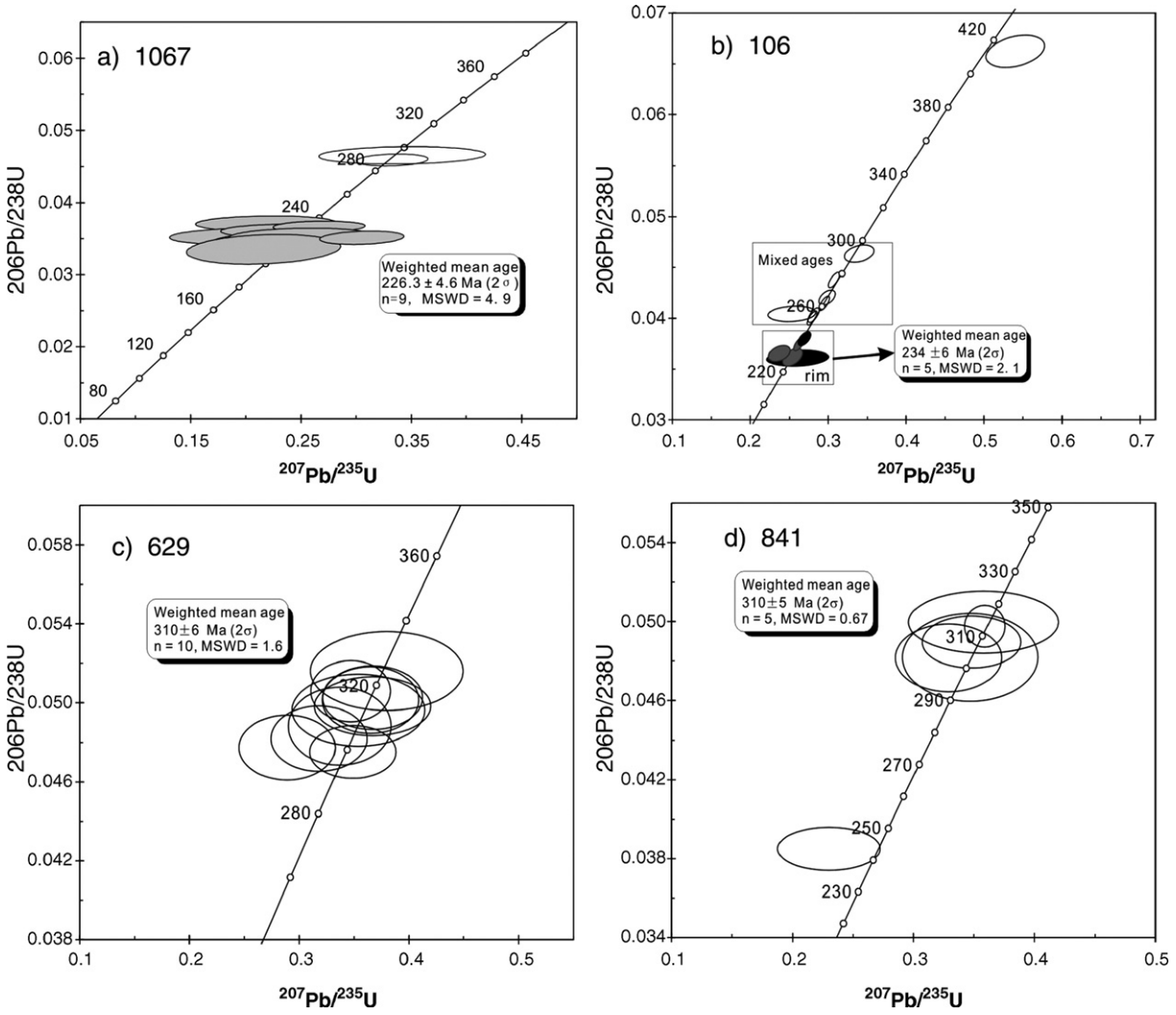

Fig. 4. Concordia diagrams showing results of individual SHRIMP 25 μm spot analyses with 2σ error ellipsoid. a. Eclogite sample 1067; b. eclogite sample 106; c. eclogite 629; d. eclogite sample 841.

absent feldspar in eclogites during the HP-UHP metamorphism. The low LREE content in rims of zircon maybe due to the dramatic growth of zoisite during HP-UHP metamorphism. Combining with rutile inclusion in the rimes of zircon, we interpret the mean 226±4.6 Ma age as dating HP-UHP metamorphism. The two core ages of 289.4±2.0 and 293.5±3.1 Ma are not a sufficient data set for constraining the age of the mafic intrusion, but can be taken as a minimum age for the protolith of the eclogite.

The zircon crystals from eclogite sample (106) are euhedral, elongate (50 to 100 μm in major dimension) and colorless (Fig. 6a, b, c, d). The CL images show that more than 50% of grains have a bright-luminescent core surrounded by a narrow dark-luminescent rim. One core analysis yields a $^{206}Pb/^{238}U$ ages of 413±6 Ma (Table 1). Because the analysis is discordant, 413±6 Ma is a minimum age for the zircon core. Five analyses of zircon rims (Table 1) yield a mean $^{206}Pb/^{238}U$ ages of 234.3±6.5 Ma (MSWD=2.9) (Fig. 3b). One rim is slightly younger (220±3 Ma) and was excluded due to suspected Pb loss. Because rims are usually less than 25 μm (the size of SHRIMP pits), mixing ages between core and rim were obtained in seven cases ($^{206}Pb/^{238}U$ ages between 253±2.9 to 292.1±3.5 Ma) (Fig. 6b, d). These data are plotted in the same concordia diagram (Fig. 4b). The trace element analyses of zircon crystals show that the content of total HREE and Y is higher in the cores (∑HREE: 1980–6408 ppm and Y: 2343–8227 ppm) than in the rims (∑HREE: 359–509 ppm and Y: 443~1153 ppm), and Eu/Eu* values are larger in the

Table 2
The trace element analyses of Zircon from eclogite (sample 1067) in western Tianshan, China

	1.1R	3.1C	4.1c	5.1R	6.1c	8.1R	9.1R	12.1R	13.1R	14.1R
La	0.02	0.05	0.05	0.01	0.03	0.01	0.01	0.02	0.01	0.04
Ce	4.54	26.16	72.2	3.53	20.11	4.52	4.55	4.29	3.78	5.52
Pr	0.02	0.41	0.22	0.02	0.1	0.02	0.02	0.02	0.01	0.02
Nd	0.13	8.15	4.96	0.56	1.55	0.32	0.23	0.13	0.13	0.26
Sm	0.6	14.69	13.58	0.9	3.49	0.79	0.54	0.74	0.6	0.86
Eu	0.42	5.08	2.45	0.398	1.01	0.5	0.352	0.39	0.326	0.38
Gd	3.2	64.86	73.85	4.26	19.4	7.05	3.05	2.33	2.44	5.12
Tb	1.29	20.98	28.88	1.23	7.84	1.2	1.103	0.823	0.813	1.61
Dy	11.11	234.74	341.33	14.89	98.45	11.34	10.42	8.34	8.26	14.43
Ho	3.4	81.59	124.3	4.57	35.64	3.48	3.01	2.12	2.14	4.39
Er	11.32	326.95	499.49	20.87	150.36	14.25	11.64	8.86	7.34	16.8
Tm	2.54	72.19	106.12	4.93	32.37	3.34	2.41	1.81	1.39	3.91
Yb	20.96	715.13	941.13	62.68	307.95	35.56	22.61	14.58	12.77	38.51
Lu	3.86	90.66	117.73	8.66	40.86	8.21	3.01	2.43	1.82	4.87
Y	104.32	2117.16	3128.94	144.74	990.24	116.46	102.06	75.42	66.90	84.73
Eu/Eu*	0.74	0.42	0.19	0.51	0.29	0.43	0.66	0.83	0.71	0.42
∑HREE	57.68	1607.1	2232.83	122.09	692.87	84.43	57.25	41.29	36.97	89.64
∑REE	63.41	1661.63	2326.29	127.5	719.16	90.59	62.94	46.75	41.81	96.71

R: rim; C: core.

rims (0.63–0.91) than in the cores (0.22–0.25) (Table 3; Fig. 5b), these suggest that the cores may be magmatic and rims may be metamorphic in origin (Rubatto, 2002; Bingen et al., 2004). Therefore, we interpret the $^{206}Pb/^{238}U$ ages of 413±6 Ma measured in one core as maximum age for the protolith of the eclogite. The zircon rims dated at 234.3±6.5 Ma are interpreted as representing eclogitic metamorphism.

The zircon from eclogite sample 629 is also euhedral, colorless and 50–100 μm in major dimension. CL images show that they have oscillatory-zoning (Fig. 6e). A few zircon grains have narrow rims that were too thin to be analyzed. A few inclusions of quartz and apatite were identified. Ten zircons selected for SHRIMP U–Pb analyses yielded $^{206}Pb/^{238}U$ ages ranging from 299±5 to 324±8 Ma with Th/U values from 0.34 to 0.55 (Table 1). These analyses plot on Concordia (Fig. 4c), and define a concordia age of 310±5 Ma (n=10). The oscillatory zoning and the relatively high Th/U of these zircon are in line with a magmatic origin (Rubatto and Gebauer, 2000). The 310±5 Ma age is thus interpret as dating the protolith of the eclogite.

The euhedral and colorless zircon crystals from eclogite sample 841 are similar to those of sample 629 (Fig. 6f). CL images show oscillatory-sector zoning, and in some cases a narrow luminescent rim is present. No mineral inclusions were found is crystals from this sample. Five analyses out of six yielded $^{206}Pb/^{238}U$ ages ranging from 303±9 to 315±6 Ma, and high Th/U values from 0.43 to 1.28 (Table 1). On the Concordia diagram, the analyses define a concordia age of 310±7 Ma (Fig. 4d), which is indistinguishable from that of sample 629 (Fig. 4c). One analysis yielded a younger age (244±4 Ma).

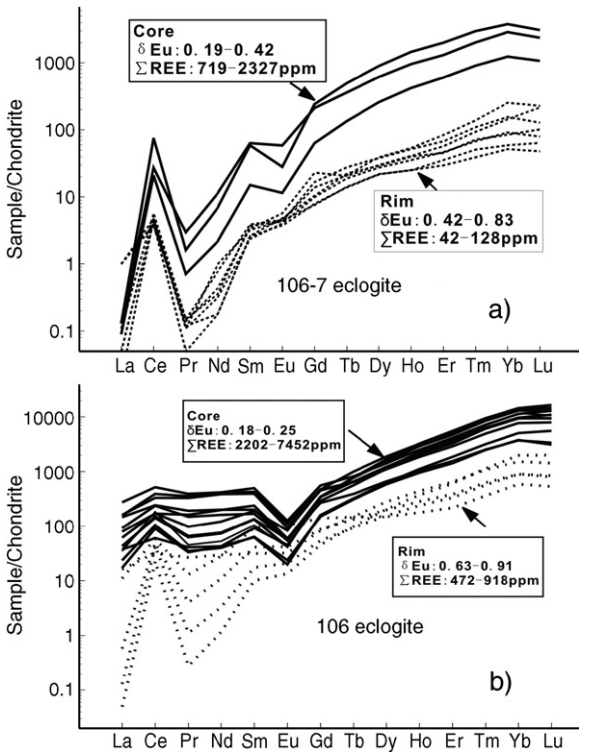

Fig. 5. Chondrite normalised REE patterns of zircon cores and metamorphic rims a) eclogite sample 1067 and b) eclogite sample 106. Normalisation after Sun and McDonough (1989).

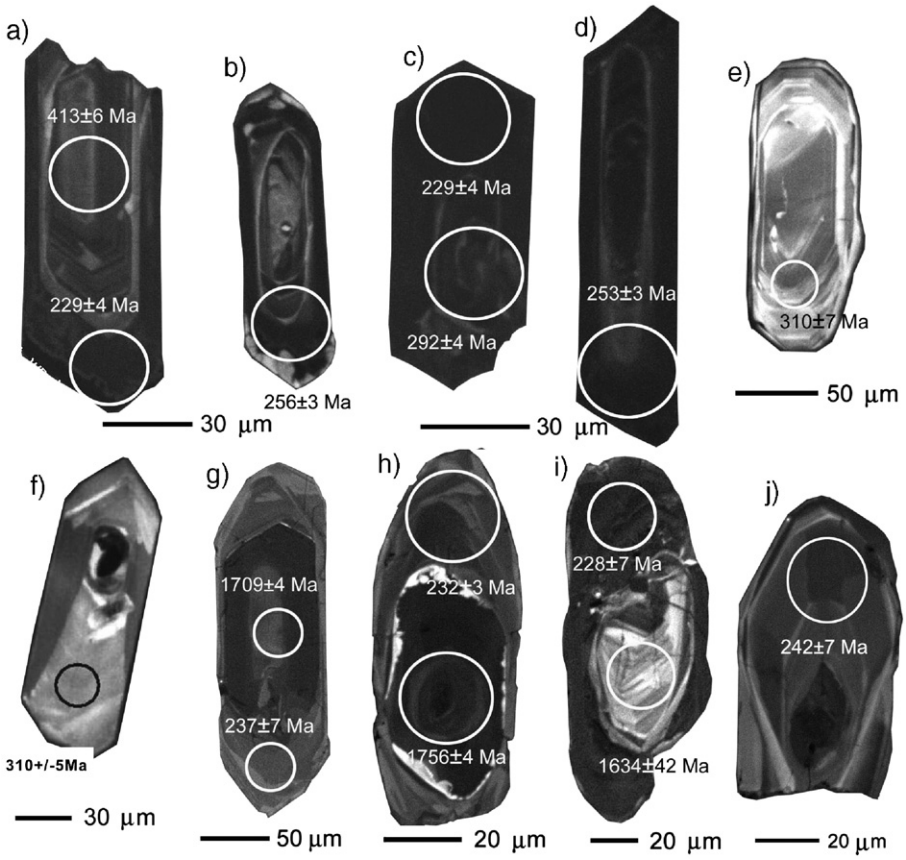

Fig. 6. Representative CL images of zircon crystals for SHRIMP U–Pb analyses from the eclogites and metapelite in Western Tianshan, China. a–d: euhedral zircon crystals with core and rim texture from eclogite sample 106; e: euhedral oscillatory zoning zircon from eclogite samples 841; f: euhedral oscillatory zoning zircon from eclogite sample 629; g–j: rounded zircon crystals from metapelites sample 111 with thick rims and oscillatory zoning in the cores.

Zircon from metapelite sample 111 is quite different from the eclogitic zircon crystals described above. In the metapelite, zircon grains are elongated, but with rounded edges and irregular crystal faces (Fig. 6g, h, i, j). Under the stereomicroscope, some zircons show a dark brown yellow core (80–100 μm across) and a colorless rim (up to 40 μm wide). CL images indicate that the subrounded cores have various CL intensity and zoning patterns, in most cases oscillatory (Fig. 6g). The variable features and the rounded shape of the core are in line with a detrital origin as expected in a sedimentary rock. The cores have sharp contacts with the rims, which show weak zoning, with irregular bands or traces of sectors. Fourteen U–Pb analyses define a discordia line that intersects the concordia curve at 1886±20 Ma and 224±25 Ma (Fig. 5e). Concordant $^{206}Pb/^{238}U$ ages were measured from 228.2±6.6 Ma to 1755.9±3.8 Ma, and the detrital core $^{207}Pb/^{206}Pb$ ages scatter between 1252±59 Ma and 1898±8.6 Ma. Four low-U rims with Th/U values from 0.02 to 0.07 analyzed yielded a weighted average age of 233±4 Ma (Fig. 7). We interpret the average age of the analyzed zircon rims as dating eclogite-facies metamorphism in agreement with the rim ages of 234±7 Ma from eclogite (sample 106) and 226±4.6 Ma age from eclogite (sample 1067). The upper intersect $^{206}Pb–^{207}Pb$ age of 1886±20 Ma is probably the mean ages of detrital inherited zircon crystals and thus geologically meaningless. The $^{206}Pb–^{207}Pb$ ages measured in the cores can be taken as indication of the crustal components present in the source of the sediment.

Because there are no index metamorphic mineral inclusions found in zircon domains beside rutile from Tianshan eclogitic rocks as mentioned above, it is hard to identify the exact age of peak HP-UHP or retrograde blueschist facies metamorphism from 226±4.6 Ma to 234±7 Ma. However, one eclogite (sample 106) and one eclogite-facies metapelite (sample 111) give the similar zircon rim ages: 233±4 Ma and 234±7 Ma, and another eclogite (sample 1067) shows 226.6±4.6 Ma age. We intend to interpret the age of 234±7 Ma as the

Table 3
The trace element analyses of zircon from eclogite (sample 106) in western Tianshan, China

	1.1c	1.2c	2.1c	3.1c	5.1c	6.1c	7.1r	7.2c	8.1r	12.1r	14.1r	15.1c	15.2c	16.1c	16.1-2c
La	13.8	12.81	3.92	15.9	4.24	54.05	5.94	13.75	4.09	0.02	0.047	33.96	29.23	59.45	58.59
Ce	149.09	176.63	22.15	160.23	28.79	233.94	31.25	58.17	56.33	21.9	41.64	227.96	163.79	318.08	375.52
Pr	9.23	6.23	1.68	8.31	3.09	26.46	3.64	5.66	1.79	0.04	0.153	20.5	22.37	45.33	48.94
Nd	55.39	37.79	11.56	48.81	18.09	143.33	21.09	30.45	20.17	0.83	2.36	115.9	141.99	276.61	296.42
Sm	31.84	24.21	8.23	25.79	9.55	46.8	7.25	14.5	21.74	2.33	4.03	39.27	55.5	91.72	98.98
Eu	4.92	3.62	1.35	3.03	1.14	5.05	2.81	1.74	9.12	1.177	1.82	4.78	5.2	8.14	9.68
Gd	108.88	106.52	34.81	77.35	40.07	106.07	25.27	49.3	42.94	14.01	16.73	106.55	82.37	139	144.75
Tb	44.11	46.28	15.11	29.56	18.5	38.11	8.78	18.86	8.58	5.77	5.53	45.3	22.74	38.3	37.53
Dy	564.08	632.17	204	386.63	253.37	456.01	107.16	236.98	57.19	78.46	59.54	643.46	254.05	468.76	423.15
Ho	218.2	251.07	86.57	151.99	104.38	193.12	37.73	95.31	15.22	31.93	20.54	278.32	89.37	183.73	158.72
Er	1014.26	1198.76	411.13	705.62	479.79	947.03	163.26	463.7	54.36	151.67	83.87	1382.52	387.78	882.42	724.84
Tm	251.2	312.34	102.05	179.86	114.71	227.71	38.77	113.62	13.01	41.05	20.47	339.11	90.67	218.71	177.47
Yb	2878.77	3366.34	1123.37	1987.71	1196.94	2408.28	377.98	1257.94	146.99	492.38	223.39	3585.75	923.51	2336.07	1916.79
Lu	410.21	494.89	177.01	291.49	180.92	419.36	54.51	212.67	20.42	76.51	32.24	629.23	129	362.62	303.42
Y	6463.74	7366.58	2343.08	4527.59	2808.03	5889.88	1152.85	2767.77	443.45	947.41	586.59	8226.47	2431.89	5644.11	4874.7
Eu/Eu*	0.24	0.22	0.24	0.24	0.18	0.22	0.63	0.20	0.91	0.63	0.68	0.23	0.24	0.22	0.25
∑HREE	5489.71	6408.37	2154.05	3810.21	2388.68	4795.69	813.46	2448.38	358.71	891.78	462.31	7010.24	1979.49	4629.61	3886.67
∑REE	5753.98	6669.66	2202.94	4072.28	2453.58	5305.32	885.44	2572.65	471.95	918.08	512.36	7452.61	2397.57	5428.94	4774.8

R: rim; C: core.

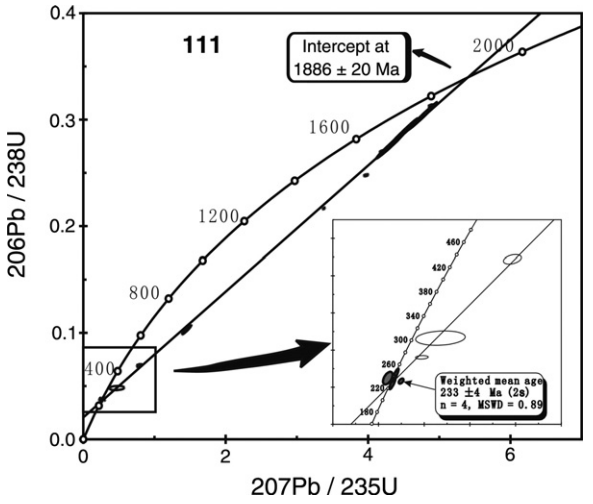

Fig. 7. Concordia diagrams showing results of individual SHRIMP 25 μm spot analyses with 2σ error ellipsoid from Omp-Gt phengite schist sample 111.

peak UHP metamorphism age and 226±4.6 Ma as blueschist facies retrograde metamorphic age. Because the eclogite (sample 1067) was overprinted by blueschist-facies metamorphism extensively.

5. Tectonic implication and discussion

The SHRIMP U–Pb ages for zircons from four eclogites and one eclogite-facies metapelite described above constrain several important geological events for this HP-UHP terrane. The time for the collision of the Chinese Western Tianshan orogenic belt represented by HP-UHP metamorphic eclogitic rocks is Triassic (234±7–226±4.6 Ma), the south Tianshan Paleo-ocean was formed before Carboniferous (>289 Ma, more likely 310±5 Ma), and some Proterozoic continental materials (1252±59–1898±8.6 Ma detrital zircon ages) took part in the Triassic collision. The tectonic evolution is schematically shown in Fig. 8 and described below.

Before the Late Carboniferous, a South Tianshan Paleo-ocean occurred between the Tarim and Yili-central Tianshan cratons (Fig. 8a). The 310±5 Ma age for the protolith of the eclogites is interpreted as the formation age of this ocean. The northward docking of the Gondwanan Karakoram–Qingtang block to the Cathaysian (Eurasian) Kunlun block was suggested to occur during the Carboniferous–Triassic in the western Kunlun area adjacent to the Chinese western Tianshan (Xiao et al., 2002). At this time, the south Tianshan paleo-oceanic crust began to subduct northward beneath the Yili-central Tianshan plate to produce arc volcanic rocks and coeval low-P granulite-facies rocks in the southern active margin of Yili-central Tianshan craton (Fig. 8b). According to SHRIMP U–Pb zircon dating of low-P granulites resulting from arc magmatic intrusion, the subduction started at about 290–280 Ma (Li and Zhang, 2004). At last, the south Tianshan oceanic and some continental crustal materials were subducted to mantle depth to form UHP metamorphic rocks (Zhang et al., 2002a,b, 2003a, 2005) then exhumated during the Early Triassic collision between the Tarim and Yili-central Tianshan plates (234±7–226±4.6 Ma) (Fig. 8c).

Recently, more and more evidences from geological and geophysical studies show that the Chinese Tianshan orogenic belt was likely formed in Mesozoic. Based on the paleomagnetic data in apparent polar wander path, Li (1990) concluded that the collision of the Tarim and Yili-central Tianshan (Kazakhstan) plate occurred after the Permian. The study of sedimentary strata shows that no extensional basin formed in the Tianshan region during that time because of the compressive setting at the Triassic (Carroll et al., 1990, 1995). The similarities of the paleontologic species and terrestrial deposits between the north and south of Tianshan orogenic belt after the Late Permian led Wang et al. (1994) to suggest that the collision and final connection between the Tarim and Yili-central Tianshan occurred during 230–292 Ma.

Based on the 245.5±0.3 Ma $^{40}Ar/^{39}Ar$ data of biotite in metagabbro from the Changawuzi dismembered ophiolite associated with HP-UHP metamorphic eclogites (Hao and Liu, 1993), Chen et al. (1999) suggested that the collision of the western Tianshan was completed at the Late Permian to Early Triassic. The stratigraphic, structural and magmatic studies revealed that the south Tianshan is entirely a Paleozoic–Triassic addition to continental crust in Kyrgyzstan, Uzbekistan and Tajikistan (Brookfield, 2002). The discovery of Late Permian radiolarian in Chinese Tianshan ophiolites, such as *Albaillella excelsa* Ishiga, Kito and Imoto, *Follicullus* sp., *Follicucullus* sp. aff. *Folicucullus bipartitus* Caridroit et De Wever made Li et al. (2001, 2005) conclude that there was a relict paleo-southern Tianshan ocean in the Late Permian in the western part of Tianshan. Recently, more and more evidences from paleomagnetic and geochronological data on the ophiolites and collisional granites along the Chinese Tianshan suture zone show that the Chinese Tianshan is an oblique collisional orogeny, produced by the clockwise rotation of the Tarim block during its northward subduction beneath the Yili-central Tianshan plate from east to west (e.g. Chen et al., 1999). The UHP metamorphism occurring at the end of the closure of relict southern Tianshan paleo-oceanic basin started in Early Permian time, in which the Tarim plate

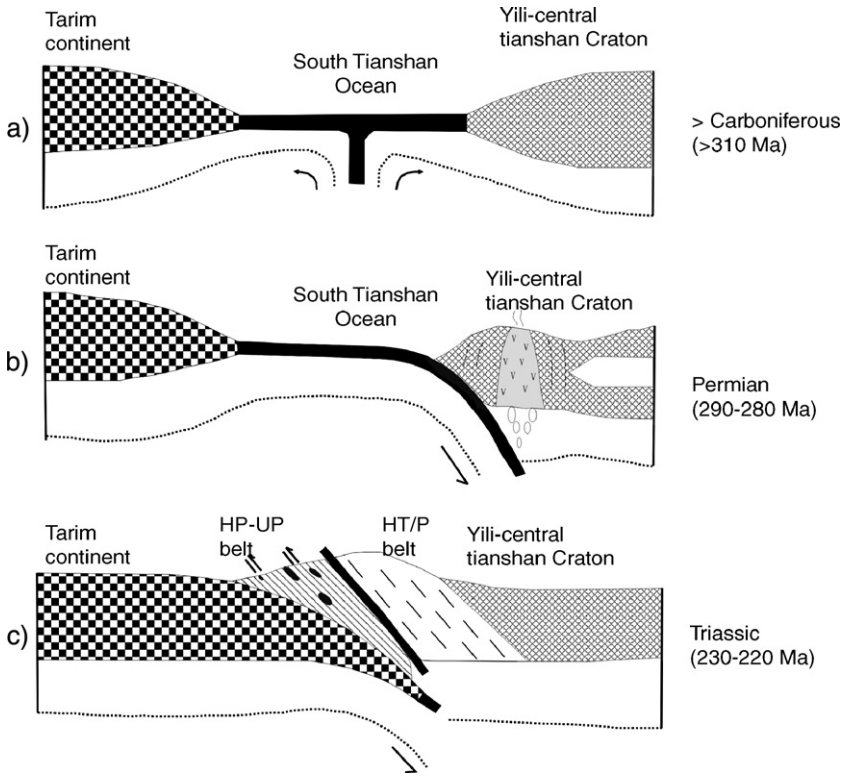

Fig. 8. Schematic cartoon showing the continental collision between the Tarim and Yili-central Tianshan (Kazakhstan) plates in Xinjiang, China. a: A South Tianshan Paleo-ocean occurred between the Tarim and Yili-central Tianshan cratons before the Late Carboniferous; b: South Tianshan paleo-oceanic crust began to subduct northward beneath the Yili-central Tianshan plate to produce arc volcanic rocks and coeval low-P granulite-facies rocks in the southern active margin of Yili-central Tianshan craton in 290–280 Ma; c: the collision between Tarim and Yili-central Tianshan plates and the formation of HP-UHP metamorphic rocks during the Early Triassic (234–226 Ma).

rotated 26° clockwise with respect to the Yili-central Tianshan plate (e.g. Li, 1990). The zircon U–Pb SHRIMP ages of 233±4–226±4.6 Ma give the strong evidence for the final closure of relict paleo-southern Tianshan ocean in the Late Permian and Mesozoic collision of Southwestern Tianshan orogenic belt in China.

Previously, most geologists have considered the Tianshan belt as Late Paleozoic based on available geologic data (Huang, 1978; Sengör et al., 1993; Wang et al., 1994). Windley et al. (1990) and Allen et al. (1992) subdivided the Chinese Tianshan orogenic belt into a south and a north collisional zone; the southern zone formed during Late Devonian to Early Carboniferous, as suggested by an unconformity along the north margin of the Tarim Block. According to the stratigraphic, structural and chemical data in volcanics, Brookfield et al. (2002) suggested that the South Tianshan in Kyrgyzstan, Tajikistan and Uzbekistan is a Paleozoic–Triassic accretionary belt. Gao et al. (2000), Gao and Klemd (2003) and Klemd et al. (2005) suggested that the western Tianshan ocean closed in the Late Paleozoic based on $^{40}Ar/^{39}Ar$ plateau ages of 401±1–344±1 Ma for glaucophane and phengite from eclogite and blueschist and one Sm–Nd isochron age of 343±44–346±3 Ma for eclogitic rocks, and Rb–Sr isochron ages of 313–302 Ma. It is known that the $^{40}Ar/^{39}Ar$ dating of HP-UHP phengite or glaucophane can be problematic due to the unknown excess argon such as in the cases of Dabie (Li et al., 1994; Wang et al., 2000; Hacker et al., 2000), Western Alps (Kelly et al., 1994; Arnaud and Kelley, 1995; Scaillet, 1996) and Himalayan HP rocks (Tonarini et al., 1993). The Sm–Nd and Rb–Sr isochron methods for dating metamorphic ages are mainly based on the isotopic equilibrium between the coexisting minerals and whole rocks in one metamorphic rock. In the case of Chinese Tianshan HP-UHP eclogites and blueschists, most of porphyroblastic garnet has compositional zonation of major elements (Gao et al., 1999; Zhang et al., 2002a) which implies that the chemical equilibrium had not reached homogeneously. As pointed out by Jahn et al. (2005) that isotopic equilibrium would not be expected to occur when chemical equilibrium is not reached.

Because the peak metamorphic temperature for Chinese western Tianshan UHP eclogitic rocks is 550–600 °C (Gao et al., 1999; Zhang et al., 2002a;) which is lower than the value of garnet Sm–Nd isotopic blocking temperature (650 °C to 850 °C) (Jagoutz, 1988; Zhou and Hensen, 1995; Burton et al., 1995;Thöni, 2002). In addition, there are so many LREE enriched and very low Sm/Nd ratios inclusion minerals such as epidote and zoisite crowded in the core of porphyroblastic garnet as mentioned above which could lower the Sm/Nd ratios in garnet and affect the isochron construction based on garnet–clinopyroxene–whole rock and other minerals (Jahn et al., 2005). Therefore, the Sm–Nd isochron method is not suitable for the dating of low temperature eclogites from Chinese Tianshan. In conclusion, thus far, no reliable metamorphic age related to the Chinese Tianshan collision event was available, although some evidences have shown that the Tianshan orogenic belt maybe formed in Early Mesozoic to Late Paleozoic. Our SHRIMP U–Pb ages of 234±7–226±4.6 Ma for the metamorphic ages of eclogite are also near to the Rb–Sr isochron age of 267 Ma obtained by Tagiri et al. (1995) in Atbashy eclogite, the westernmost Tianshan in Kyrghyzstan, and support the Early Triassic orogenic belt for western Tianshan, China.

6. Conclusions

The study of SHRIMP U–Pb dating combining with Laser ICP-MS zircon trace element analyses shows that zircon from four eclogites yield magmatic ages of 310–413 Ma in the cores and one metapelite contained detrital zircon cores as old as 1886±20 Ma, zircon rims with REE pattern of metamorphic origin reveal the HP-UHP metamorphic ages of 233±4–226±4.6 Ma. The geochronologial data in this paper suggest that a South Tianshan paleo-ocean was developed between the Tarim continent and the Yili-central Tianshan Craton before the Carboniferous (>310 Ma), during the Permian–Triassic subduction and continental collision, oceanic basalts underwent HP/UHP metamorphism. The southwestern Tianshan orogenic belt in China was formed in Mesozoic.

Acknowledgment

This study was supported by National Nature Science Foundation of China (Grants 40325005, 40228003), TRAPOYT of MOE, China and the Laser-ICP-MS Analysis Fund from the Key Laboratory of Continental Dynamics in Northwest University of China to the first author. This manuscript has had critical review by S. Graham. We thank Yaoling Niu for his encouragement and suggestions. The authors are grateful to two anonymous journal referees for their constructive and detailed comments.

References

Abdrakhmatov, K., Aldazhanov, S., Hager, B., Hamburger, M., Herring, T., Kalabaev, K., Makarov, V., Molnar, P., Panasyuk, S., Prilepin, M., Reilingert, R., Sadykakasov, I., Souter, B., Trapeznikov, T., Tsurkov, V., Zubovich, A., 1996. Relatively recent construction of the Tien Shan inferred from GPS measurements of present-day crustal deformation rates. Nature 384, 450–453.

Ai, Y., 2005. The geochemical and geochronological study on the HP-UHP metamorphic eclogites from Southwestern Tianshan, China. Ph.D. thesis of Peking University (in Chinese with English abstract), p 243.

Ai, Y., Zhang, L., Li, X., Qu, J., 2005. The geochemical characteristics and tectonic implications of the UHP eclogites and blueschists, Southwestern Tianshan, China. Progress in Natural Science 11,1346–11,1356 (in Chinese with English abstract).

Allen, M., Windley, B., Zhang, C., 1992. Palaeozoic collisional tectonics and magmatism of the Chinese Tienshan, central Asia. Tectonophysics 220, 89–115.

Allen, M., Vincent, S., Wheeler, P., 1999. Late Cenozoic tectonics of the Kepingtag thrust zone: interactions of the Tien Shan and Tarim Basin, Northwestern China. Tectonics 18, 639–654.

Arnaud, N.O., Kelley, S., 1995. Evidence for excess Ar during high pressure metamorphism in the Dora Maira (west Alps, Italy), using an ultra-violet laser ablation microprobe $^{40}Ar/^{39}Ar$ technique. Contributions to Mineralogy and Petrology 121, 1–11.

Bingen, B., Austrheim, H., Whitehouse, M., Davis, W., 2004. Trace element signature and U–Pb geochronology of eclogite-facies zircon, Bergen Arcs, Caledonides of W Norway. Contributions to Mineralogy and Petrology 147, 671–680.

Black, L.P., Kamo, S.L., Allen, C.M., Aleinikoff, J.M., Davis, D.W., Korscha, R.J., Foudoulis, C., 2003. TEMORA 1: a new zircon standard for Phanerozoic U–Pb geochronology. Chemical Geology 200, 155–170.

Brookfield, M., 2002. Geological development and Phanerozoic crustal accretion in the western segment of the southern Tien Shan (Kyrgyzstan, Uzbekistan and Tajikistan). Tectonophysics 328, 1–14.

Burton, K., Kohn, M., Cohen, A., O'Nions, R., 1995. The relative diffusion of Pb, Nd, Sr and O in garnet. Earth and Planetary Science Letters 133, 199–211.

Carroll, A., Liang, Y., Graham, S., Xiao, X., Hendrix, M., Chu, J., Mcknight, L., 1990. Junggar basin, northwest China: trapped Late Paleozoic ocean. Tectonophysics 181, 1–14.

Carroll, A., Graham, S., Hendrix, M., Ying, D., Zhou, D., 1995. Late Paleozoic tectonic amalgamation of northwestern China: sedimentary record of the northern Tarim, northwestern Turpan, and southern Junggar basins. Geological Society of America Bulletin 107, 571–594.

Chen, S., Lu, H., Jia, D., Cai, D., Wu, S., 1999. Closing history of the southern Tianshan oceanic basin, western China: an oblique collisional orogeny. Tectonophysics 302, 23–40.

Claoué-Long, J.C., Compston, W., Roberts, J., Fanning, C.M., 1995. Two Carboniferous ages: a comparison of SHRIMP zircon dating with conventional zircon ages and $^{40}Ar/^{39}Ar$ analysis. In: Berggren, W.A., Kent, D.V., Aubrey, M.P., Hardenbol, J. (Eds.), Geochronology Time Scales and Global Stratigraphic Correlation. SEPM (Society for Sedimentary Geology), Special Publication, vol. 54, pp. 3–21.

Compston, W., Williams, I.S., Meyer, C., 1984. U–Pb geochronology of zircon from lunar breccia 73217 using a sensitive high mass-resolution ion microprobe. Journal of Geophysical Resources 89, 525–534.

Compston, W., Williams, I.S., Kirschvink, J.L., Zhang, Z., 1992. Zircon U–Pb ages for the Early Cambrian time-scale. Journal of the Geological Society of London 149, 171–184.

Gao, J., 1997. The discovery of eclogites and its tectonic implication, Southwest Tianshan. Chinese Bulletin of Sciences 42, 737–740 (in Chinese with English abstract).

Gao, J., Klemd, R., 2003. Formation of HP-LT rocks and their tectonic implications in the western Tianshan Orogen, NW China: geochemical and age constraints. Lithos 66, 1–22.

Gao, J., Zhang, L., Wang, Z., et al., 1997. Metamorphic minerals and metamorphism evolution of western Tianshan high pressure belt. Acta Petrologica and Mineralogica 16, 244–254 (in Chinese with English abstract).

Gao, J., Klemd, R., Zhang, L., Wang, Z., Xiao, X., 1999. PT path of high-pressure metamorphic rocks and its tectonic implication in western Tianshan, northwest China. Journal of Metamorphic Geology 17, 621–636.

Gao, J., Zhang, L., Liu, W., 2000. The Ar^{40}/Ar^{39} age record of formation and uplift of the blueschists and eclogites in the western Tianshan Mountains. Chinese Science Bulletin 45, 1047–1052.

Hacker, B., Ratschbacher, L., Webb, L., McWilliams, M., Ireland, T., Calvert, A., Dong, S., Wenk, H., Chateigner, D., 2000. Exhumation of ultrahigh-pressure eclogite in east central China: late Triassic–early Jurassic tectonic unroofing. Journal of Geophysical Research 105, 13339–13364.

Hao, J., Liu, L., 1993. Ophiolite mélange time and tectonic evolution model in south Tianshan area. Scitica Geologica Sinica 28, 93–95 (in Chinese with English abstract).

Huang, T.K., 1978. An outline of the tectonic characteristics of China. Eclogae Geologicae Helveticae 71, 611–635.

Jagoutz, E., 1988. Nd and Sr systematics in an eclogite xenolith from Tanzania: evidence from frozen mineral equilibria in the continental lithosphere. Geochimica et Cosmochimica Acta 52, 1285–1293.

Jahn, B.-m., Liu, X., Yui, T., Morin, N., Coz, B.-le., 2005. High-pressure/ultrahigh-pressure eclogites from the Hong'an Block, East-Central China: geochemical characterization, isotope disequilibrium and geochronological controversy. Contributions to Mineralogy and Petrology 149, 499–526.

Kelly, S., Arnaud, N., Okay, A., 1994. Anomalously old Ar–Ar ages in high-pressure metamorphic terrains. Mineralogical Magazine 58, 468–469.

Klemd, R., 2003. Ultrahigh-pressure metamorphism in eclogites from the western Tianshan, China, comments. American Mineralogist 88, 1153–1156.

Klemd, R., Brocker, M., Hacker, B., Gao, J., Gans, P., Wemmer, K., 2005. New age constraints on the metamorphic evolution of the high-pressure/low temperature belt in the Western Tianshan Mountains, NW China. Journal of Geology 113, 157–168.

Li, Y.P., 1990. An apparent polar wander path from the Tarim block, China. Tectonophysics 181, 31–41.

Li, Q., Zhang, L., 2004. The PT path and geological significance of low-pressure granulite-facies metamorphism in Muzhaerte, south-west Tianshan, Xinjiang, China. Acta Petrologica Sinica 20, 583–594 (in Chinese with English abstract).

Li, S., Wang, S., Chen, Y., Zhou, H., Zhang, Z., Liou, G., Qiou, J., 1994. Excess argon in phengite of eclogite: evidence from comparing dating of eclogite by Sm–Nd, Rb–Sr, and $^{40}Ar/^{39}Ar$ isotope methods. Chemical Geology 112, 343–350.

Li, Y., Song, W., Mai, G., Zhou, L., Hu, J., Shang, X., 2001. The Kuche foreland basin of Tarim craton and its relation to Southern Tianshan orogenic belt. Xinjiang Petroleum Geology 22, 376–381 (in Chinese).

Li, Y., Sun, L., Wu, H., Zhang, G., Wang, G., Huang, Z., 2005. Permo-Carboniferous radiolarians from the Wupata'erkan group, Western South Tianshan, Xinjiang, China. Acta Geologica Sinica 79, 16–23 (in Chinese).

Liu, X., Gao, S., Lin, H., Hattendort, B., Gunther, D., Chen, L., 2002. Analyses of 42 major and trace elements in glass standard reference materials by 193 nm LA-ICPMS. Acta Petrologica Sinica 18, 408–418 (in Chinese with English abstract).

Ludwig, K.R., 2002. SQUID 1.02, a user's manual, Berkeley Geochronology Center Special Publication 2, 2455 Ridge Road, Berkeley, CA 94709, USA 22.

Paces, J.B., Miller, J.D., 1993. U–Pb ages of the Duluth complex and related mafic intrusions, northeastern Minnesota: geochronologic insights into physical petrogenetic, paleomagnetic and tectono-magmatic processes associated with the 1.1 Ga mid-continent rift system. Journal of Geophysical Research 98, 13,997–14,013.

Rubatto, D., 2002. Zircon trace element geochemistry: partitioning with garnet and the link between U–Pb ages and metamorphism. Chemistry Geology 184, 123–138.

Rubatto, D., Gebauer, D., 2000. Use of cathodoluminescence for U–Pb zircon dating by ion microprobe: some examples from the Western Alps. In: Pagel, M., Barbi, V., Blanc, P., Ohnenstetter, D. (Eds.), Cathodoluminescence in geosciences. Springer, Berlin Heidelberg New York, pp. 373–400.

Scaillet, S., 1996. Excess $^{40}Ar^{39}Ar$ transport scale and mechanism in high pressure phengite: a case study from an eclogitized metabasite of the Dora Maira nappe, western Alps. Geochimica et Cosmochimica Acta 60, 1075–1090.

Sengör, A., Natal'in, B., Burtman, V., 1993. Evolution of the Altaid tectonic collage and Paleozoic crustal growth in Eurasia. Nature 364, 299–307.

Stern, R.A., 1998. High-resolution SIMS determination of radiogenic tracer-isotope ratios in minerals. In: Cabri, L.J., Vaughan, D.J. (Eds.), Modern Approaches to Ore and Environmental Mineralogy. Mineralogical Association of Canada, Short Course Series, vol. 27, pp. 241–268.

Sun, S.-s., McDonough, W.F., 1989. Chemical and isotopic systematics of oceanic basalt: implications for mantle composition and processes. In: Saunders, A.D., Norry, M.J. (Eds.), Magmatism in the Ocean Basins. Geol. Soc. Lon. Spec. Publ., vol. 42, pp. 313–345.

Tagiri, M., Yano, T., Bakirov, A., Nakajima, T., Uchiumi, S., 1995. Mineral parageneses and metamorphic paths of ultrahigh-pressure eclogites from Kyrghyzstan Tien-Shan. Island Arc 4, 280–292.

Tonarini, S., Villa, I.M., Oberl, F., 1993. Eocene age of eclogite metamorphism in Pakistan Himalaya: implications for India Eurasia collision. Terra Nova 5, 13–20.

Thöni, M., 2002. Sm–Nd isotope systematics in garnet from different lithologies (Eastern Alps): age results, and an evaluation of potential problems for garnet Sm–Nd chronometry. Chemistry Geology 185, 255–281.

Volkava, N.I., Budanov, V.I., 1999. Geochemical discrimination of metabasalt rocks of the Fan-Karategin transitional blueschist/greenschist belt, South Tianshan, Tajikistan, seamount volcanism and accretionary tectonics. Lithos 47, 201–216.

Wang, B., Lang, Z., Li, X., Qu, X., Li, T., Huang, C., Cui, X., 1994. Comprehensive Survey of Geological Sections in The West Tianshan of Xinjiang, China. Science Press, Beijing, p. 202 (in Chinese with English abstract).

Wang, S., Ge, N., Sang, H., 2000. Genesis of excess argon in phengite and significance of ^{40}Ar–^{39}Ar age spectra for omphacite: a case study on UHP eclogite of south Dabie Terrain, China. Chinese Science Bulletin 45, 1345–1351.

Williams, I.S., 1998. U–Th–Pb geochronology by ion microprobe. In: McKibben, M.A., Shanks, W.C. (Eds.), Applications of microanalytical techniques to understanding mineralizing processes. Reviews in Economic Geology, pp. 1–35.

Windley, B., Allen, M., Zhang, C., Zhao, Z., Wang, G., 1990. Paleozoic accretion and Cenozoic redeformation of the Chinese Tien Shan Range, central Asia. Geology 18, 128–131.

Xiao, W., Windley, B., Chen, H., Zhang, G., Li, J., 2002. Carboniferous–Triassic subduction and accretion in the western Kunlun, China: implications for the collisional and accretionary tectonics of the northern Tibetan Plateau. Geology 30, 295–298.

Zhang, L., Gao, J., Ekerbair, S., Wang, Z., 2000. Low temperature eclogite facies metamorphism in Western Tianshan, Xinjiang. Science in China. Series D 44, 85–96 (in Chinese with English abstract).

Zhang, L., Ellis, D.J., Jiang, W., 2002a. Ultrahigh pressure metamorphism in western Tianshan, China, part I: evidences from the inclusion of coesite pseudomorphs in garnet and quartz exsolution lamellae in omphacite in eclogites. American Mineralogist 87, 853–860.

Zhang, L., Ellis, D.J., Williams, S., Jiang, W., 2002b. Ultrahigh pressure metamorphism in western Tianshan, China, part II: evidence from magnesite in eclogite. American Mineralogist 87, 861–866.

Zhang, L., Ellis, D.J., Williams, S., Jiang, W., 2003a. Ultrahigh pressure metamorphism in eclogites from the Western Tianshan, China. Reply. American Mineralogist 88, 1157–1160.

Zhang, L., Ellis, D.J., Arculus, R.J., Jiang, W., Wei, C., 2003b. "Forbidden zone" subduction of sediments to 150 km depth — the reaction of dolomite to magnesite+aragonite in the UHPM metapelites from western Tianshan, China. Journal of Metamorphic Geology 21, 523–529.

Zhang, L., Song, S.G., Ai, Y.L., Liou, J.G., 2005a. Relict coesite exsolution in omphacite from western Tianshan eclogites, China. American Mineralogist 89, 180–186.

Zhang, L., Ai, Y., Li, Q., Li, X., Song, S., Wei, C., 2005b. The formation and tectonic evolution of UHP metamorphic belt in Southwestern Tianshan, Xinjiang. Acta Petrologica Sinica 21, 1029–1037 (in Chinese with English abstract).

Zhou, B., Hensen, B., 1995. Inherited Sm/Nd isotope components preserved in monazite inclusions within garnets in leucogneiss from East Antarctica and implications for closure temperature studies. Chemistry Geology 121, 317–326.